NIH Public Access
Author Manuscript
Neuroimage. Author manuscript; available in PMC 2015 December 01.

Published in final edited form as:
Neuroimage. 2014 December ; 103: 290–302. doi:10.1016/j.neuroimage.2014.09.032.

3D GABA imaging with real-time motion correction, shim update and reacquisition of adiabatic spiral MRSI

Wolfgang Bogner[1,2,*], **Borjan Gagoski**[3,*], **Aaron T Hess**[4], **Himanshu Bhat**[5], **M. Dylan Tisdall**[1], **Andre J.W. van der Kouwe**[1], **Bernhard Strasser**[2], **Małgorzata Marjańska**[6], **Siegfried Trattnig**[2], **Ellen Grant**[3], **Bruce Rosen**[1], and **Ovidiu C Andronesi**[1,#]

[1]Athinoula A. Martinos Center for Biomedical Imaging, Department of Radiology, Massachusetts General Hospital, Harvard Medical School, Boston, MA, USA

[2]MRCE, Department of Biomedical Imaging and Image-guided Therapy, Medical University Vienna, Vienna, Austria

[3]Fetal-Neonatal Neuroimaging & Developmental Science Center, Boston Children's Hospital, Harvard Medical School, Boston, MA, USA

[4]Department of Cardiovascular Medicine, John Radcliffe Hospital, University of Oxford Centre for Clinical Magnetic Resonance Research, Oxford, UK

[5]Siemens Healthcare, Charlestown, MA

[6]Center for Magnetic Resonance Research and Department of Radiology, University of Minnesota, Minneapolis, Minnesota, USA

Abstract

Gamma-aminobutyric acid (GABA) and glutamate (Glu) are the major neurotransmitters in the brain. They are crucial for the functioning of healthy brain and their alteration is a major mechanism in the pathophysiology of many neuro-psychiatric disorders.

Magnetic resonance spectroscopy (MRS) is the only way to measure GABA and Glu non-invasively *in vivo*. GABA detection is particularly challenging and requires special MRS techniques. The most popular is MEscher-GArwood (MEGA) difference editing with single-voxel Point RESolved Spectroscopy (PRESS) localization. This technique has three major limitations: a) MEGA editing is a subtraction technique, hence is very sensitive to scanner instabilities and motion artifacts. b) PRESS is prone to localization errors at high fields (≥3T) that compromise

© 2014 Elsevier Inc. All rights reserved.

[#]Corresponding author. Phone +1-617-643-6864, Fax +1-617-726-7422, ovidiu@nmr.mgh.harvard.edu (O.C.Andronesi).
[*]authors contributed equally

Parts of this study were presented at:
- Bogner, W. et al., *Real-time motion and B0-corrected 3D-MRSI with selective reacquisition for MEGA editing of GABA in the brain*. ISMRM, 2014, Milan, Italy

Publisher's Disclaimer: This is a PDF file of an unedited manuscript that has been accepted for publication. As a service to our customers we are providing this early version of the manuscript. The manuscript will undergo copyediting, typesetting, and review of the resulting proof before it is published in its final citable form. Please note that during the production process errors may be discovered which could affect the content, and all legal disclaimers that apply to the journal pertain.

NIH-PA Author Manuscript
NIH-PA Author Manuscript
NIH-PA Author Manuscript

NIH-PA Author Manuscript

NIH-PA Author Manuscript

NIH-PA Author Manuscript

accurate quantification. c) Single-voxel spectroscopy can (similar to a biopsy) only probe average GABA and Glu levels in a single location at a time.

To mitigate these problems, we implemented a 3D MEGA-editing MRS imaging sequence with the following three features: a) Real-time motion correction, dynamic shim updates, and selective reacquisition to eliminate subtraction artifacts due to scanner instabilities and subject motion. b) Localization by Adiabatic SElective Refocusing (LASER) to improve the localization accuracy and signal-to-noise ratio. c) K-space encoding via a weighted stack of spirals provides 3D metabolic mapping with flexible scan times.

Simulations, phantom and *in vivo* experiments prove that our MEGA-LASER sequence enables 3D mapping of GABA+ and Glx (Glutamate + Gluatmine), by providing 1.66 times larger signal for the 3.02 ppm multiplet of GABA+ compared to MEGA-PRESS, leading to clinically feasible scan times for 3D brain imaging.

Hence, our sequence allows accurate and robust 3D-mapping of brain GABA+ and Glx levels to be performed at clinical 3T MR scanners for use in neuroscience and clinical applications.

Keywords

neurotransmitter; GABA; glutamate; MEGA editing; magnetic resonance spectroscopy; LASER; prospective motion correction; real-time correction; spiral imaging; frequency drift correction; reacquisition

1. Introduction

Gamma-aminobutyric acid (GABA) and glutamate (Glu) are the major inhibitory and excitatory neurotransmitters in the brain, respectively (Agarwal and Renshaw, 2012; Novotny et al., 2003). They play an important role in healthy brain function (Baslow and Guilfoyle, 2007; Muthukumaraswamy et al., 2009; Northoff et al., 2007) and the pathophysiology of several major neurological and psychiatric diseases (Agarwal and Renshaw, 2012; Novotny et al., 2003). Significant changes in neurotransmitters can be observed during drug treatments (e.g., anti-epileptic drugs) (Petroff et al., 1999) or during brain development and aging (Gao et al., 2013; Pouwels et al., 1999). Hence, there is a strong interest in the neuroscience and neuropsychiatric communities to measure the *in vivo* levels of these neurotransmitters.

Magnetic resonance spectroscopy (MRS) is the only non-invasive technique to measure the local concentrations of GABA and Glu in the brain (Mullins et al., 2014; Novotny et al., 2003). Glu is fairly abundant in the brain (6–12 mM), but J-coupling and overlap with glutamine (Gln) complicate quantification (Xin et al., 2008). The GABA concentration, even in cortical gray matter, is low (~1–2 mM) compared to the other metabolites that dominate the MR spectrum (Agarwal and Renshaw, 2012; Novotny et al., 2003). Additionally, all three GABA resonances (i.e., 3.01 ppm, 2.28 ppm, 1.88 ppm) overlap with more intense signals originating from Glu, N-acetylaspartate (NAA), creatine (Cr), phosphocreatine (PCr), and macromolecules (MM). These aspects make reliable quantification of GABA difficult with conventional (non-editing) MRS sequences.

NIH-PA Author Manuscript

NIH-PA Author Manuscript

NIH-PA Author Manuscript

Several MRS methods for GABA editing have been proposed based on: i) J-difference spectroscopy (Hetherington et al., 1998; Keltner et al., 1996; Mescher et al., 1998; Rothman et al., 1993), ii) multiple quantum filtering (Choi et al., 2006; Keltner et al., 1997), iii) selective Hartmann-Hahn transfer (Choi et al., 2005), and iv) multidimensional J-resolved MRS or 2D-COSY and 2D-TOCSY (Andronesi et al., 2012a; Andronesi et al., 2010a; Thomas et al., 2003; Thomas et al., 2001).

J-difference spectroscopy is quoted (Puts and Edden, 2012) to have the highest SNR for GABA detection. The higher SNR, the conceptual simplicity, and the availability on commercial scanners made the MEscher-GArwood (MEGA) Point RESolved Spectroscopy (PRESS), so called MEGA-PRESS (Mescher et al., 1998), the most common implementation of J-difference MRS for localized GABA detection (Mullins et al., 2014). MEGA-PRESS edits the GABA signal at 3.01ppm by removing the much larger overlapping total tCr (Cr + PCr) signal. Two spectra are acquired interleaved and subsequently subtracted: i) an EDIT-ON spectrum with selective refocusing of the H3–H4 J-coupling evolution, and ii) an EDIT-OFF spectrum without selective refocusing of the H3–H4 J-coupling evolution. Nevertheless, the measured GABA signal is typically contaminated by co-edited macromolecules (MM), referred to as GABA+ (Mescher et al., 1998; Mullins et al., 2014), unless more careful strategies are taken to reduce MM contaminations (Henry et al., 2001). Also the measured Glu signal is contaminated by glutamine and glutathione and, thus, often abbreviated as Glx. Nevertheless, the difference (OFF-ON) spectrum allows accurate and stable quantification of GABA and good quantification of Glx (Henry et al., 2011).

Several technical limitations of MEGA-PRESS exist at the moment. First, there are problems resulting from PRESS localization. Chemical shift displacement errors (CSDE) or sensitivity to B1 inhomogeneity reduce the editing efficiency, in particular at high (≥3T) magnetic field strengths (B_0) (Edden and Barker, 2007; Kaiser et al., 2007; Mullins et al., 2014; Near et al., 2013). Combination of MEGA editing with improved localization approaches such as semi-LASER (Localized Adiabatic Spin-Echo Refocusing, Arteaga de Castro et al., 2013), PRESS with inner volume saturation (Edden and Barker, 2007), PRESS +4 (Kaiser et al., 2007), and SPECIAL (SPin ECho, full Intensity Acquired Localized, Near et al., 2011) have been introduced to partially overcome these problems.

Second, for difference methods such as MEGA-PRESS, subject motion and scanner instabilities result in subtraction artifacts that may bias or if severe prevent quantification (Evans et al., 2013; Mullins et al., 2014; Waddell et al., 2007). Retrospective phase/frequency correction of individual averages with discarding of corrupted spectra have been proposed to reduce subtraction artifacts, but these corrections are typically limited to single-voxel spectroscopy (SVS) (Evans et al., 2013; Mullins et al., 2014; Waddell et al., 2007).

Motion-control methods using interleaved navigators for SVS MEGA-PRESS editing of GABA have been demonstrated previously (Bhattacharyya et al., 2007). However, the interleaved navigators were used to detect repetitions that are corrupted by motion and discard them from averaging, hence compromising sensitivity and not correcting in real-time

NIH-PA Author Manuscript

NIH-PA Author Manuscript

NIH-PA Author Manuscript

for changes in localization and frequency. The real-time frequency adjustment was shown for MEGA-PRESS (Zhu et al., 2011), but without real-time motion correction.

A further limitation in GABA detection is spatial coverage. The majority of GABA investigations by MRS were performed via SVS in ~6–10 min (Bogner et al., 2010; Gao et al., 2013; Mullins et al., 2014; Petroff, 2002; Puts and Edden, 2012; Rothman et al., 1993). Larger brain coverage has been shown so far only as single slice 2D-MR spectroscopic imaging (MRSI) of GABA+ using phase encoding in combination with double quantum filtering in ~25 min (Choi et al., 2006), MEGA-editing in ~17 min (Zhu et al., 2011) and by selective homo-nuclear polarization transfer in ~19 min (Pan et al., 2013). To our knowledge robust 3D GABA imaging based on MEGA-editing has not been published, yet. The prospect of 3D GABA+ mapping is mainly hindered by long scan times due to the low levels of GABA requiring averaging for adequate SNR which increase the likelihood of subtraction artifacts due to scanner instabilities and subject motion.

Recently, we have shown that accurate, fast, and robust 3D mapping of the major brain metabolites is possible at 3 T in ~4 min by combining LASER localization, spiral encoding, and real-time Shim, and Motion Correction (ShMoCo) (Bogner et al., 2013).

The aim of our current study was, to expand the capabilities of this 3D-MRSI sequence by implementing MEGA-editing with fully adiabatic low-power/large-bandwidth LASER localization, acquisition weighted stack of spirals, and real-time motion correction improved by additional selective reacquisition of corrupted spectra. This new 3D MEGA-LASER editing spiral spectroscopic sequence with Reacquisition, Shim, and Motion Correction (ReShMoCo) was evaluated in simulations, as well as in phantoms and volunteers on clinical 3 T MR systems for its feasibility to provide fast and robust high resolution volumetric mapping of GABA+ and Glx in the human brain.

2. Materials and Methods

2.1. Scanner hardware

All measurements were performed on two 3T TIM Trio MR scanners (Siemens Healthcare, Erlangen, Germany) using the body coil for transmission and a 32-channel head coil (Siemens Healthcare, Erlangen, Germany) for signal reception. Multi-channel MRSI data were optimally combined based on coil sensitivity profiles (Roemer et al., 1990) as determined from MRI prescans. Measurements were performed at two different sites, Martinos Center for Biomedical Imaging, MGH, Harvard Medical School and the MRCE, Department of Biomedical Imaging and Image-guided Therapy, Medical University Vienna.

2.2. Sequence design

2.2.1. Spatial localization—VOI localization in our 3D-MRSI measurements was achieved by a B_1^+-insensitive LASER sequence as previously described (Andronesi et al., 2012b; Bogner et al., 2013) with a non-selective adiabatic half passage (AHP) excitation pulse (HS8 modulation; duration 4 ms; bandwidth 5 kHz) and three pairs of selective Gradient Offset Independent Adiabatic (GOIA) pulses (W16,4 modulation; duration 3.5 ms; bandwidth 20 kHz). All adiabatic pulses were run with a B_1^+ safety margin of 10% above

NIH-PA Author Manuscript

NIH-PA Author Manuscript

NIH-PA Author Manuscript

the adiabatic threshold. Slice profiles for pulses used in PRESS and LASER localization are shown in Supplementary Fig 1.

Time efficient data acquisition was achieved by spiral encoding in the (k_x,k_y)-plane using constant-density spiral trajectories (Adalsteinsson et al., 1998). Phase encoding gradients were superimposed over the last MEGA-spoiler gradient of the LASER sequence to encode along the z-direction. This resulted in a cylindrical 3D-coverage of the k-space by a stack of spirals. To improve the point spread function (PSF) and optimize the SNR per unit time, weighted acquisition was implemented in the z-direction using a cosine shaped window function.

2.2.2. MEGA editing—To keep the echo time (TE) short, MEGA editing was implemented in the LASER localization scheme using a pair of 60 Hz Gaussian refocusing pulses with 14.8 ms duration. The spoiler gradients (20 mT/m amplitude and 3 ms duration) surrounding both editing pulses were arranged in a similar way as originally proposed by Mescher et al. (Mescher et al., 1998). The position of the MEGA editing pulses was chosen to optimize the editing efficiency based on simulations (Fig 1).

EDIT-ON/OFF spectra were acquired in an interleaved fashion to account for frequency drift throughout the acquisition. During odd-numbered acquisitions the MEGA editing pulses refocused the $^3CH_2$ resonance of GABA at 1.9 ppm, which are weakly coupled to the triplet peak at 3.02 ppm (EDIT-ON). During even-numbered acquisitions, the refocusing was applied symmetrically to the other side of the water peak, *in vivo* at 4.7 + (4.7 – 1.9) = 7.5 ppm (EDIT-OFF) and had no effect on the GABA resonances.

To improve the localization, additional 2-step phase cycling was implemented to eliminate artifacts from incoherent echo pathways. Note that the most inner loop was the interleaved acquisition of EDIT-ON/OFF, followed by phase cycling, spiral encoding, phase encoding and averaging. The ON/OFF spectra were stored separately and subtracted at the end of the online sequence reconstruction.

2.2.3. Motion/B_0 correction with selective reacquisition—For the detection of real-time motion and B_0-field changes a dual-contrast, multi-shot 3D-EPI navigator (vNav) was inserted prior to the water suppression module of the 3D-MRSI sequence. This vNav determined the required shim, frequency, and head pose changes for the entire volume of interest (VOI) for each TR. In particular, because of the narrow band selective pulses used for MEGA editing and WET water suppression updating the shims and frequency is highly desirable. More details on the used vNav setup were described previously (Bogner et al., 2013; Hess et al., 2011).

Zhu et al. proposed to perform frequency alignment for 2D-MRSI only on pairs of EDIT-ON/OFF spectra (Zhu et al., 2011) and also SVS reports suggest that pairwise frequency alignment is superior to individual alignment (Evans et al., 2013). Similarly, using our real-time approach we found pair updating superior and we update our frequency, B_0 shims, and VOI/FOV position only every second TR (pair-by-pair, i.e., once for each pair of EDIT-ON/OFF spectra). Furthermore, to account for possible motion during acquisition of one of

NIH-PA Author Manuscript

NIH-PA Author Manuscript

NIH-PA Author Manuscript

the EDIT-ON/OFF interleaves, we additionally implemented a selective reacquisition of corrupted data pairs (Tisdall et al., 2012). If either the head translation or rotation between EDIT-ON and EDIT-OFF was larger than three times the standard deviation (i.e., 0.4 mm or 0.4°) of the motion normally observed during a static *in vivo* scan, the affected EDIT-ON/OFF pair was discarded and immediately reacquired in the following two TRs. This procedure reduced the motion artifacts further and, importantly, preserved the SNR. Reacquisition was limited to a maximum of 25% of the total scan time. The alternative of discarding motion corrupted repetitions is generally not possible for MRSI, since this means removing k-space points.

The total vNav block, including navigator acquisition (612 ms) and online processing (150 ms), was ~760 ms long. Navigator acquisition, updating, reacquisition, and all of the image reconstruction was fully implemented and integrated on the scanner.

2.3. Simulations

In order to optimize the timing of the MEGA-LASER editing sequence, we performed quantum mechanical simulations using the GAMMA library (Smith et al., 1994) and the spin definition from Near et al. (Near et al., 2013). The position and time interval between the MEGA pulses (i.e., the total TE is split into three time intervals TE1/TE2/TE3 by the MEGA pulses) was varied by changing the number of GOIA-W(16,4) pulses before (N1), between (N2), and after (N3) the two MEGA pulses (Figs 1,2). SNR gain and sensitivity to B_1^+ inhomogeneities were compared between MEGA-LASER and MEGA-PRESS.

The evolution of the density matrix under time-dependent Hamiltonians was calculated using a piecewise approach with a 10 μs time step. The same RF and gradient pulse shapes, modulations, and sample points that were used experimentally were reproduced in the simulations (Fig 1). Simulations for LASER were performed using experimentally used parameters. The PRESS localization employed a hamming-filtered four-lobes sinc (HSINC4) excitation pulse of 2.6 ms/3.36 kHz/0.97 kHz (duration/bandwidth/B_{1max}) and two MAO refocusing pulses (Mao et al., 1988) of 5.2 ms/1.15 kHz/1.05 kHz (duration/bandwidth/B_{1max}). To account for the effects of chemical shift displacement errors and the related 4-compartment effect a number of 400 slice isochromats were calculated and integrated along each spatial dimension.

In both MEGA-LASER and MEGA-PRESS simulations, the same Gaussian shaped MEGA editing pulses (i.e., 60 Hz bandwidth and 14.8 ms duration) and same MEGA gradient spoilers (i.e., 20 mT/m amplitude and 3 ms duration) were used. With these parameters a TE of 68 ms is possible for both MEGA-LASER and MEGA-PRESS. The MEGA-LASER pulse sequence with optimal timing and pulse combination is shown in Fig 1. The timing of MEGA-PRESS was chosen exactly according to the original MEGA scheme (Mescher et al., 1998). Spectra were simulated for a spectral window of 10 ppm and 2048 sampling points.

2.4. Sequence testing

2.4.1. Phantom tests—A cylindrical multi-compartment spectroscopy phantom was used to evaluate the performance of ReShMoCo during motion. In the center of this phantom, we

NIH-PA Author Manuscript

NIH-PA Author Manuscript

NIH-PA Author Manuscript

positioned a rectangular compartment of 5×5×5 cm^3 containing brain metabolites at close to physiological concentrations: 3 mM GABA, 12.5 mM NAA; 10 mM Cr; 3 mM choline (Cho); 7.5 mM *myo*-inositol (mI); 12.5 mM Glu; and 5 mM lactate (Lac); 1 ml/L of Gd-DTPA (Magnevist®, Bayer) to obtain *in vivo*-like T_1 relaxation. The central compartment was surrounded by eight Falcon tubes filled with 10% ethanol or water mixed with Gd-DTPA. All compartments were fixed inside a larger cylindrical container filled with water. This multi-compartment phantom had enough structure (Fig 3) to be tracked during motion by the vNav.

A step-by-step right-left rotation (i.e., in total 45°) was performed during the acquisition of the central k-space points since most of the signal is acquired at this time period and the strongest motion induced artifacts can be expected. The right-left rotation provided also small displacements in the up-down and head-foot directions, which mimic typical head movements.

The editing efficiency for both MEGA-LASER and MEGA-PRESS sequences, including SNR and uniformity of excitation, was investigated with a uniform spherical phantom (16 cm diameter) that contained 20 mM GABA and 20 mM Glu.

The following 3D-MRSI measurement parameters were used in phantom tests: TR/TE 1600/68 ms and FOV 200×200×200 mm^3. For the ReShMoCo test a 10×10×10 matrix (8 cm^3 isotropic voxels) interpolated to a 16×16×16 matrix VOI 50×50×50 mm^3, bandwidth 1.11 kHz, two temporal and one angular interleaves, ten weighted averages, four dummy scans, and acquisition time (TA) 5:26 min were used. Five measurements were performed: 1) static with ReShMoCo; 2) static without ReShMoCo; 3) motion with ReShMoCo; 4) motion with ShMoCo; 5) motion without any correction. For testing the editing efficiency, we acquired a 20×20×16 matrix interpolated to 32×32×16, VOI 100×100×50 mm^3, bandwidth 1.25 kHz, two temporal and four angular interleaves, one average, four dummy scans, TA 6:56 min. Two static measurements with ReShMoCo were performed, one for MEGA-LASER and one for MEGA-PRESS. Except for the volume localization (i.e., either LASER or PRESS) all the other parameters of the sequences were identical, including the vNav, MEGA editing pulses and spiral encoding.

2.4.2. Volunteer tests—For *in vivo* validation, six healthy volunteers (three males, three females; 31±1years of age) were scanned. Of these, five performed predefined motion tasks. One subject was scanned with three different 3D MEGA-LASER protocols (i.e., shorter scans with lower resolution and longer scans with higher resolution) to illustrate the flexibility of our new sequence. Institutional Review Board approval and written, informed consent were obtained.

To ensure accurate placement of the VOI, 3D T_1-weighted images were acquired using an MEMPRAGE sequence (van der Kouwe et al., 2008) and were re-sliced to be used as localizers. Subsequently, five 3D-MRSI scans were performed in which the subject was either instructed to stay still or to perform a predefined motion task.

NIH-PA Author Manuscript

NIH-PA Author Manuscript

NIH-PA Author Manuscript

For testing the performance of real-time correction, the following five measurements were performed: 1) static with ReShMoCo; 2) static without ReShMoCo; 3) motion with ReShMoCo; 4) motion with ShMoCo; 5) motion without any correction. The most likely motion patterns typically observed during neuro-MRI scans are chin up-down and chin right-left rotations (Bhattacharyya et al., 2007). Thus, for our *in vivo* tests a combination of both movements (right-left rotation ±6–7° and up-down rotation ±4–5°) that was fairly easy to memorize was defined. An example of real-time coordinate tracking is shown in Figure 5.

After each motion experiment, the volunteers were instructed to return to their original position. Localizer images were repeatedly acquired to validate that the subjects had indeed returned to their initial position. To further ensure the reproducibility of initial head position relative to the VOI/FOV adjustment, AutoAlign was run prior to each 3D-MRSI scan (Benner et al., 2006; van der Kouwe et al., 2005). Gradient echo imaging based shimming was repeated after each motion scan to set the initial B_0 shim. All subjects were briefed and trained in a short test session prior to the actual movement experiments. Audio cues were given to additionally improve the reproducibility of the motion tasks.

For all *in vivo* motion testing 3D-MRSI measurement parameters were adjusted as listed in Table 1 (Protocol I with 8 cm^3 nominal resolution).

In one additional healthy volunteer four 3D-MRSI scans were performed with three different spatial resolutions, to illustrate the flexibility of our sequence to provide excellent 3D GABA mapping in both short measurement time for standard (lower) resolution, as well as longer scan times for higher spatial resolution. Sequence parameters for these optimized 3D-MRSI protocols are listed in Table 1.

2.5. Data evaluation and statistical analysis

2.5.1. Spectral processing and evaluation—Spectral processing of all voxels within the VOI plus one additional row of border voxels was performed automatically by LCModel software (Provencher, 2001) using simulated basis sets for two kinds of spectra: EDIT-OFF and difference. The basis set for EDIT-OFF spectra included 21 commonly included brain metabolites (i.e., alanine, ascorbic acid, aspartate, Cr, GABA, Glu, Glu, glycine, 2-hydroxyglutarate (2HG), mI, *scyllo*-inositol, Lac, PCr, phosphoethanolamine, taurine, NAA, phosphocholine, glutathione, glycerol, glycerophosphocholine, N-acetyl aspartyl glutamate). The basis sets for difference spectra included the five major metabolites that were affected by the editing pulse applied at 1.9 ppm (i.e., NAA, GABA, Glu, Gln, and 2HG). The basis sets were simulated using the pulses and MEGA-LASER schema illustrated in Fig 1.

The metabolic signal intensity ratio GABA+/Glx was computed along with spectral quality measures and fitting quality parameters (i.e., signal-to-noise ratios (SNR) and Cramer-Rao lower bounds (CRLB) of GABA+). CRLBs were obtained from LCmodel, but SNR was calculated in frequency domain via a Matlab script and defined as the respective signal amplitude divided by the standard deviation of the noise in the frequency range from 6–8ppm. The results were plotted as metabolic signal amplitude maps, ratio maps and spectral quality/fitting quality maps. Note, for LCModel fitting no pre-processing apodization filter

NIH-PA Author Manuscript

NIH-PA Author Manuscript

NIH-PA Author Manuscript

was used. Exponential multiplication of difference spectra was used in some figures only for visualization purposes.

Localization accuracy and spectral quality were evaluated qualitatively (i.e., visual assessment of spectral quality and metabolic maps) and quantitatively (i.e., SNR, metabolic signal intensity ratios, CRLB, signal integral, contamination of subtraction spectra). Contamination was assessed by estimating the SNR of the subtraction error of the 3.22 ppm choline resonance (Waddell et al., 2007).

2.5.2. Statistical analysis—Statistical analysis was performed and plots were created using SPSS (v15.0; Chicago, Ill).

Only voxels inside the VOI and excluding ventricles were further evaluated (i.e., the SNR of NAA was too low outside this mask).

To asses global changes in spectral quality and quantification, the mean and the standard deviation of the neurotransmitter signal intensity ratio GABA+/Glx, the SNR of GABA+, the contamination (i.e., SNR of choline subtraction artifacts), and CRLB of GABA+ were determined inside this mask. To determine the number of voxels that had substantial subtraction artifacts, we applied an SNR threshold of SNR > 3 to filter out measured contamination that could be considered noise. The percentage of contaminated voxels was determined.

Paired t-tests across all voxels and subjects were performed to compare the reference standard (i.e., static scan without any correction) and ReShMoCo scans with all remaining scans. A $p < 0.05$ was considered statistically significant.

3. Results

3.1. Simulations

3.1.1. LASER timing optimization—In Fig 2a, the signal of the GABA edited peak at 3 ppm is compared for different positions and distances of the MEGA pulses. The MEGA pulses divide the total TE in three time intervals (i.e., TE1/TE2/TE3 containing N1/N2/N3 GOIA pulses). The highest edited signal was obtained for the situation when the MEGA pulses were separated by half of the echo time (TE2=34 ms) in the second part of the echo. This corresponds to the MEGA-LASER having three GOIA-W(16,4) pulses before the first MEGA pulse (N1=3), and the remaining three GOIA-W(16,4) pulses between the two MEGA pulses (N2=3, N3=0). This pulse combination of MEGA-LASER is similar to the timing of the MEGA-PRESS sequence (Mescher et al., 1998).

3.1.2. LASER vs. PRESS—In Fig 2b, the optimal MEGA-LASER and MEGA-PRESS sequences are compared using simulations. MEGA-LASER offered significant signal gain for GABA compared to MEGA-PRESS. The total integrated signal was 2.03 times higher in MEGA-LASER compared to MEGA-PRESS. The signal gain in each of the three GABA main peaks was different: 1) the largest upfield peak (i.e., 2.95 ppm) was 1.52 times higher in MEGA-LASER than MEGA-PRESS; 2) the lowest central peak (i.e., 3.01 ppm) was 4.36

NIH-PA Author Manuscript

NIH-PA Author Manuscript

NIH-PA Author Manuscript

times higher in MEGA-LASER; and 3) the downfield peak (i.e., 3.07 ppm) was 1.21 times higher in MEGA-LASER.

The performance of MEGA-LASER and MEGA-PRESS with respect to B_1^+ inhomogeneities is illustrated in Fig 2c,d. When varying the B_1^+ amplitude by ±10% around the optimal value, the variance in the integrated signal of the edited GABA multiplet was low (i.e., 3–7%) for MEGA-LASER (Fig. 2c), but high (i.e., 12%–28%) for MEGA-PRESS (Fig. 2d). The shape of the GABA multiplet in MEGA-LASER was preserved, while in MEGA-PRESS the multiplet shape changed. In particular, the outer multiplet peaks decreased and the inner peak increased when B_1^+ deviated from the optimum value in MEGA-PRESS.

At 3 T, the CSDE between GABA resonances at 1.9 ppm and 3 ppm is 0.6% for GOIA-W(16,4) pulses, 4% for HSINC4 and 11.7% for MAO pulses. The common excited volume of H3 and H4 GABA resonances is therefore 98% for MEGA-LASER, but only 75% for MEGA-PRESS. Slice profiles of pulses involved in LASER and PRESS localization can be seen in Supplementary Fig. 1, showing more uniform and sharper excitation of pass-band for GOIA pulses, and the absence of sidebands in the out-of-band regions.

3.2. Phantom measurements

3.2.1. LASER vs. PRESS—The experimental results agree with the improvement of MEGA-LASER over MEGA-PRESS predicted by simulations. The overall GABA signal integral within the VOI (excluding border voxels) was 1.66 times larger for MEGA-LASER (in a.u. 43±5) than for MEGA-PRESS (26±5). For certain voxels, especially in the middle of VOI, the changes in the subtracted GABA integral were even larger (~2 times higher in MEGA-LASER). The B_1^+ variation in the phantom as measured by a B_1^+ mapping sequence was similar to *in vivo* conditions (i.e., 85±9° within the quantified VOI).

The B_1^+ variability within our homogeneous phantom caused substantial variations in both signal amplitude and shape of the GABA triplet at 3 ppm. For MEGA-PRESS, we observed a loss in total integrated GABA signal, both, in the center and towards the borders of the phantom (Fig 4), as caused by either too high or too low B_1^+, respectively, as well as slice profiles (see Supplementary Fig. 2). On the other hand, MEGA-LASER provided homogeneous editing over the whole phantom (Fig 4).

3.2.2. Reacquisition, Shim, Motion Correction—Our evaluations show that movement of the localization phantom (Supplementary Fig 2) during the MEGA-LASER acquisition led to strong contamination of signal outside the VOI (i.e., alcohol) and in addition substantial subtraction artifacts for the edited GABA signal in difference spectra, if no correction was performed (Fig 3). The use of ShMoCo removed major contamination, but some residual subtraction artifacts remained. ReShMoCo improved the data quality of motion affected scans even further, but a difference relative to static scans remained. On the other hand both static phantom scans (with and without ReShMoCo) had similarly excellent spectral quality (Fig 3).

NIH-PA Author Manuscript

NIH-PA Author Manuscript

NIH-PA Author Manuscript

3.3. Volunteer measurements

3.3.1. Reacquisition, Shim, Motion Correction—Spectral quality parameters of five different measurements performed on volunteers (n=5) (static without correction, static with ReShMoCo, motion without correction, motion with only ShMoCo, and motion with ReShMoCo) are listed in table 2. The performed motion task as tracked by the vNav (Fig 5) was not strong enough to significantly reduce the spectral quality and fitting of EDIT-OFF scans, but difference spectra were more sensitive to motion artifacts (Fig 6). For scans with ReShMoCo, the contamination SNR was significantly lower (2.0±1.2) (Fig 7) compared to scans without correction (2.5±1.4; $p < 0.001$) or scans with ShMoCo (2.6±1.5; $p < 0.001$). When counting only voxels with contamination of SNR > 3, the percentage of voxels with substantial subtraction artifacts was reduced in each volunteer when comparing noMoCo (4%–64%) to ReShMoCo (4%–30%) (Fig 8). The contamination for the static case and motion case both with ReShMoCo were not different ($p = 0.23$), but the static case with ReShMoCo had lower contamination than the static case without correction ($p < 0\ 01$), the motion case with no correction ($p < 001$), and even the motion case with ShMoCo ($p < 001$). GABA+/Glx signal intensity ratios were higher for the noMoCo cases (0.86±0.08) compared to ShMoCo (0.84±0.08; $p<0.01$) and ReShMoCo (0.81±0.07; $p<0.01$). Uncorrected motion artifacts lead to an average overestimation of GABA+ SNR (12.9±5.4 to 11.5±5.0) by 12% compared to scans with ReShMoCo. In all cases results with ReShMoCo were better than static scans without correction (Fig 6).

3.3.2. Scan time vs. spatial resolution—The SNR/CRLB values measured for GABA + within the VOI of the three different measurement protocols were 10±4/12±3% for 8 cm^3 isotropic resolution, 8±3/14±4% for 3 cm^3, and 5±4/20±5% for 1 cm^3. Interpolated 3D GABA+ maps illustrate the excellent fitting precision achieved for all three suggested protocols (Fig 9 and Supplementary Fig 2). During the scans a frequency drift of 8 Hz for 8 cm^3, 12 Hz for 3 cm^3, and 18 Hz for 1 cm^3 was observed and corrected via our automated real-time B_0 shim and frequency update.

4. Discussion

In this study, we introduced an improved MEGA editing MRSI method for robust 3D mapping of GABA+ and Glx in the human brain for use on clinical 3 T MR scanners. Simulations, as well as phantom and *in vivo* scans provide evidence of the advantages compared to commonly available MEGA-editing approaches. Our method combines three highly optimized sequence modules: a) LASER selection provides improved B_1^+ insensitive localization and lower CSDE which approximately doubled the GABA+ signal amplitude compared to MEGA-PRESS; b) 3D spatial encoding by acquisition weighted stack of spirals provided a flexible protocol choice ranging from short standard resolution to longer high resolution neurotransmitter mapping; c) Real-time motion- and B_0-correction with selective reacquisition of corrupted data ensured robust measurements even during longer scans with incompliant subjects or scanner instabilities.

NIH-PA Author Manuscript

NIH-PA Author Manuscript

NIH-PA Author Manuscript

4.1. LASER selection and editing efficiency

So far, the bulk of MEGA-editing sequences used for investigations of GABA levels in the human brain were using PRESS localization (Bogner et al., 2010; Gao et al., 2013; Mullins et al., 2014; Petroff, 2002; Rothman et al., 1993), as was originally proposed (Mescher et al., 1998), and similar MEGA-PRESS implementations already exist on all major vendor platforms (Marjanska et al., 2013; Near et al., 2013). This was a logical choice since PRESS is still the most widely available MRS sequence on clinical MR scanners (Kreis, 2004; Mullins et al., 2014), despite its known shortcomings that include sensitivity to B_1^+ errors, poor selection profiles, and large CSDEs (Kreis, 2004). For MEGA editing, in particular, B_1^+ errors and CSDEs, are the cause of additional limitations including (spatial) large variations in the detected GABA multiplet pattern (Edden and Barker, 2007; Mullins et al., 2014; Near et al., 2013; Waddell et al., 2007), which substantially decrease the practically achievable editing efficiency and compromise quantification. Several studies found a significant loss in GABA signal amplitude (i.e., 24–43%) due to the CSDE-related 4-compartment effect, when using MEGA-PRESS (Edden and Barker, 2007; Kaiser et al., 2008). CSDEs and the related signal loss scales linearly with the static magnetic field strength.

Several sequence approaches were, therefore, proposed to reduce the sensitivity to B_1^+ inhomogeneities and compartment effects (e.g. semi-LASER and PRESS-IVS) (Arteaga de Castro et al., 2013; Edden and Barker, 2007). At 7 T, Arteaga de Castro et al. introduced a semi-LASER sequence as a combination of non-adiabatic excitation and high-bandwidth adiabatic Frequency Offset Corrected Inversion (FOCI) pulses to reduce B_1^+ errors and compartment effects (Arteaga de Castro et al., 2013).

In contrast, our proposed full-LASER selection uses only adiabatic pulses and is, therefore, even less sensitive to B_1^+ inhomogeneities. Low-power adiabatic GOIA refocusing pulses also provide superior selection profiles similar to FOCI (Arteaga de Castro et al., 2013) but with significantly less (45%) B1max requirements, and more than a magnitude lower CSDEs than PRESS (Andronesi et al., 2010b), thereby minimizing any problems arising from compartment effects or SAR. Although full LASER localization with six refocusing pulses was applied, our optimized MEGA-LASER module uses very short GOIA pulses (i.e., 3.5 ms) compared to previously applied FOCI pulses (i.e., 6.7 ms (Arteaga de Castro et al., 2013)) and a spoiler readjustment that allowed identical TE settings as commonly used for MEGA-PRESS (i.e., TE/TE2 = 68/34 ms) and shorter than previously shown for MEGA with semi-LASER (i.e., 74 ms). Therefore, no additional T_2 losses were introduced. Rather, the opposite is the case. Due to spin locking effects spins do not undergo T_2 decay during train of adiabatic GOIA pulses, which will decrease the overall relaxation-related signal losses compared to non-adiabatic PRESS (Deelchand et al., 2014; Michaeli et al., 2002). In addition there is less diffusion weighting with shorter GOIA pulses. The combination of all of these results in increased SNR. Both our simulations and phantom measurements show the SNR improvement. Our MEGA-LASER sequence provided a significantly improved GABA signal integral (2.03 and 1.66 times as high as MEGA-PRESS in simulations and phantoms, respectively, assuming the same TE of 68 ms) even if B_1^+ amplitudes were

NIH-PA Author Manuscript

NIH-PA Author Manuscript

NIH-PA Author Manuscript

perfectly adjusted. This additional SNR can be either used to shorten measurement times or translated to higher spatial resolution.

The most notable difference between MEGA-PRESS and MEGA-LASER was the amplitude of the central GABA peak (i.e., much larger in MEGA-LASER), which is a property of the editing sequence and not an artifact due to subtraction or flip angle errors as documented for MEGA-PRESS (Near et al., 2013). Different triplet patterns were also observed previously even for different implementations of MEGA-PRESS on different vendor platforms.

Because of the adiabatic volume localization, MEGA-LASER is more stable and compensates much better for B_1^+ field inhomogeneities. The resulting stability of the multiplet shape is beneficial for spectral fitting of experimental data with basis sets (e.g., using LCModel).

4.2. Accelerated 3D spatial encoding

Robust MEGA editing of GABA requires a minimum of four measurement repetitions for two phase cycles and acquisition of EDIT-ON and OFF interleaved spectra. This is not limiting the minimum measurement times of SVS MEGA-PRESS sequences (i.e., typically performed in 6–17 min scan time (Mullins et al., 2014; Puts and Edden, 2012)), but leads to prolonged minimum scans times, if phase-encoded 2D-MRSI editing of GABA is performed (i.e., ~17 min (Zhu et al., 2011)). Consequently, extending the spatial encoding in the third spatial dimension is not feasible within reasonable scan times, unless the slow phase encoding is replaced by accelerated spatial encoding techniques such as a spiral readout (Adalsteinsson et al., 1998) or (P)EPSI (Maudsley et al., 2009; Posse et al., 1995).

In this study, we speed up our 3D mapping of GABA+ by time-efficient spiral encoding. By using spiral readouts, MRSI acquisitions can be accelerated by a factor of 50 or more compared to conventional phase encoding. For clinically useful protocols some of the available acceleration can be traded off for increased SNR by performing additional averages (Andronesi et al., 2012b). This allows a flexible choice of imaging matrix and scan time, as illustrated well in our study. To make full use of this flexibility, we additionally implemented acquisition weighting to improve the point spread function in the z-direction. This also optimized the SNR per unit time compared to conventional averaging.

With the substantial SNR gain available due to improved LASER localization, acquisition weighting, and most recent coil technology (i.e., 32-channel receive coil) we were, on the one hand, able to achieve a rough 3D mapping of a 10×10×10 matrix (i.e., 8 cm^3 resolution) within scan times similar to the shortest previously reported for MEGA-PRESS SVS sequences (i.e., ~8 min (Puts and Edden, 2012)). On the other hand, our sequence also allowed robust high-resolution GABA+/Glx mapping (i.e., 20×20×20 matrix; 1 cm^3 resolution) in ~24 min scan time with good anatomical correlation. High resolution mapping, in particular, was ensured by an optimized real-time motion correction module that additionally compensates for temporal scanner instabilities (Bogner et al., 2013). Apart from that, spiral encoding itself is less sensitive to motion artifacts and successful

NIH-PA Author Manuscript

NIH-PA Author Manuscript

NIH-PA Author Manuscript

combination of spiral encoded 3D-MRSI with real-time motion correction has been shown previously (Bogner et al., 2013).

4.3. Real-time motion and B_0 correction

It is well known that subject motion and scanner instabilities during MEGA-PRESS sequences do not only lead to additional line broadening and associated SNR loss (e.g. ~10% (Waddell et al., 2007)), but even more importantly, to significant subtraction errors that are the cause of substantial overestimation and variability in quantified GABA+ signals (Evans et al., 2013; Puts and Edden, 2012; Waddell et al., 2007). For SVS, storing each readout event separately, and performing pairwise retrospective frequency and phase alignment along with selective rejection of corrupted data pairs, has been widely accepted as an efficient way to reduce the errors caused by subject motion and frequency drift (Evans et al., 2013). Although the subtraction errors may be reduced, the localization error cannot be undo in postprocessing. However, there is no clear consensus which resonance should be used as internal frequency/phase reference. Referencing based on NAA of subtraction spectra (Terpstra et al., 2003), on Cr of EDIT-OFF spectra (Waddell et al., 2007), on the suppressed water signal of EDIT-OFF spectra (Bhattacharyya et al., 2007), and on non-suppressed water acquired via additional navigators (Zhu et al., 2011) were proposed. Although, no direct comparison of all methods has been reported in a single study, some studies suggest that the more elaborate frequency correction based on unsuppressed water acquired via an interleaved navigator should lead to the most robust frequency correction for both SVS (Bhattacharyya et al., 2007) and MRSI (Zhu et al., 2011), respectively.

It is important to note that frequency/phase alignment in MRSI cannot be performed without an additional navigator. In contrast to SVS, the signal following each MRSI excitation is spatially encoded. This additional encoding introduces phase modulations that make simple post-processing frequency/phase alignment impossible.

Although several real-time motion corrections methods exist for SVS (Hess et al., 2011; Keating and Ernst, 2012; Zaitsev et al., 2010), so far none of the methods proposed for correction of MEGA editing data, include an actual updating of the VOI or FOV to account for subject motion.

Most of the above mentioned real-time corrections and retrospective frequency/phase alignment methods cannot be easily applied to MRSI acquisitions. Although updating of global frequency/phase using an additional navigator can somewhat improve the spectral quality for MEGA-PRESS 2D-MRSI (Zhu et al., 2011), it was noted that head motion in particular, causes spatially variable frequency changes that cannot be fully corrected in all brain regions at once using a single global frequency update, in particular for large VOIs. Additional B_0 shim updates are required (Bogner et al., 2013; Hess et al., 2012; Lange et al., 2012). This is consistent with our observations. For typical head rotation, changes in 1^{st}-order shims by 2–3 Hz/cm can easily cause a frequency change of ±10–15 Hz close to the borders of a large VOI, even if the mean (global) frequency change over the whole VOI is only ±2–3 Hz.

NIH-PA Author Manuscript

NIH-PA Author Manuscript

NIH-PA Author Manuscript

Our real-time frequency/phase correction approach is similar to other studies that are using an interleaved navigator based on non-suppressed water (Bhattacharyya et al., 2007; Zhu et al., 2011). However, instead of acquiring a free induction decay that summarizes the spatially variable frequency changes in a single global frequency change, we spatially encoded this signal by inserting a volumetric EPI navigator prior to water suppression. This vNav provides two 3D magnitude/phase images of different TE before each excitation to monitor shim, frequency, and head pose changes for the entire VOI in real-time. Our approach has, therefore, two major advantages for MEGA-editing MRSI: (a) Both, VOI and FOV are "following" the subject's head in real-time with sub-millimeter precision using the magnitude images of the shorter echo (Tisdall et al., 2012). (b) Frequency updates are not restricted to a single global value, but via B_0 fieldmapping obtained from the phase images of both echoes the dynamic shim updates accounts also for local variability in frequency changes.

MEGA editing is much more sensitive to motion artifacts than conventional MRS techniques. Only a few rapid motion incidents are enough to cause differences between EDIT-ON and EDIT-OFF spectra leading to substantial subtraction errors (Bhattacharyya et al., 2007). This is particularly true in MRSI scans, if motion occurs during the acquisition of the k-space center, where the bulk of the signal is acquired. In MEGA edited SVS all acquired averages contain the same spectral/spatial information and, hence, corrupted data can be easily identified and rejected retrospectively at the expense of lower SNR. It is obvious that retrospective removal of corrupted data during MRSI would lead to missing spatial encoding steps, which would cause substantial errors in localization. Therefore, it was necessary to expand the motion correction capabilities of our previously presented 3D-MRSI sequence (Bogner et al., 2013) by a real-time identification and immediate reacquisition of corrupted data.

Unfortunately, our scanner software allows only frequency updating of integers. Hence, even similar reference frequencies (e.g., < 0.01 Hz difference), between EDIT-ON and EDIT-OFF can be rounded in an unfavorable way, thereby causing an increased frequency difference (i.e., 1 Hz). Assuming a reasonably good shim with Cr linewidth of 5–10 Hz, this rounding effect can exacerbate subtraction errors. Thus, we chose to perform no update between EDIT-ON and EDIT-OFF scans. This approach is in agreement with that previously proposed by other studies (Zhu et al., 2011). To prevent subtraction artifacts due to head motion between the acquisition of the EDIT-ON and EDIT-OFF paired spectra, we alternatively implemented a selective reacquisition of corrupted data pairs (Tisdall et al., 2012). The rejection criterion for acquired data was a maximum head motion (i.e., > 0.4 mm translation or >0.4° rotation).

Thereby, our real-time motion correction approach can correct well for both head motion and scanner frequency instabilities even during longer scans performed on incompliant subjects.

4.4. Limitations

GABA and Glu concentrations in grey matter are twice as high as in white matter (Jensen et al., 2005). Yet, our VOI selection limits investigations only to a rectangular box, which

NIH-PA Author Manuscript

NIH-PA Author Manuscript

NIH-PA Author Manuscript

complicates detection of these neurotransmitters in the cortex. Although, this is a limitation of most commonly available MRSI techniques (Kreis, 2004), there are alternative approaches with more brain coverage allowing detection of brain metabolites in cortical areas (Adalsteinsson et al., 1998; Bilgic et al., 2013; Bogner et al., 2012; Maudsley et al., 2009) and were applied successfully even to MEGA-edited 2D-MRSI (Zhu et al., 2011). Full brain coverage MRSI requires extremely good lipid suppression and/or lipid removal to eliminate the ringing of very strong lipid signals coming from bone marrow and subcutaneous fat which dominate the signal of brain metabolites. Further improvement of our sequence may eventually provide “whole brain” 3D mapping of GABA+ and Glu covering also most cortical GM areas.

Our preliminary results show also that 8-min 3D-MRSI scans are feasible, but with a spatial resolution that has very limited anatomical correspondence, while ~24min scans show already very promising anatomical features. Further optimization, as well as software (cite) and hardware (cite) improvement could eventually shorten scan times to provide the same anatomical detail also in ~8min. However, compared to the mainstream of neuroscience research that uses single voxel MRS techniques for *in vivo* GABA measurements we believe that the three MRSI protocols that we demonstrate here present clear advantages.

GABA+ and Glx are MM and Gln contaminated signals of GABA and Glu. This is not a problem if MM contaminations are constant in amplitude, as is typically assumed (Mullins et al., 2014). However, MM contamination may increase due to frequency changes caused by either scanner instabilities or motion. This can be a significant problem, as shown in our study. Improved editing pulses and higher frequency dispersion at ultra-high field MR scanners could reduce these problems (Puts and Edden, 2012; Terpstra et al., 2002).

Although we could significantly reduce the contamination of subtraction spectra, our results indicate that other sources of contamination apart from rigid head motion may exist in some of the subjects (e.g., breathing, pulsation). Further improvements, such as higher order B_0 shim updates and more accurate frequency updates (i.e., not limited by the scanner hardware to 1^{st} order shim terms and frequency updates not rounded to integers) could also further reduce subtraction artifacts and lead to a full recovery of spectral quality.

MEGA editing is an extremely powerful approach for investigating the GABAergic inhibition in the healthy brain and the pathophysiology of major neurological and psychiatric diseases. In this study we only investigated the robust 3D mapping of brain GABA+ and Glx, but other highly interesting applications for our sequence exist such as MEGA editing of 2HG (Andronesi et al., 2012c) and lactate (Arteaga de Castro et al., 2013) in brain tumors, or GSH (Terpstra et al., 2003) in neurological disorders.

Future sequence improvements, and advances in hardware technology will further facilitate the robust 3D mapping of GABA and Glu for investigations in neuroscience and clinical routine and add to the widespread application of this technique.

NIH-PA Author Manuscript

NIH-PA Author Manuscript

NIH-PA Author Manuscript

5. Conclusion

MEGA editing via a spiral-encoded 3D-LASER-MRSI sequence with real-time ReShMoCo is a powerful tool for accurate, fast, and robust 3D mapping of neurotransmitters on clinical 3 T MR scanners. This will further promote the use of MEGA-editing MRSI for neuroscience and routine clinical applications.

Supplementary Material

Refer to Web version on PubMed Central for supplementary material.

Acknowledgments

This study was supported by the Austrian Science Fund (FWF): KLI-61 and J3302-B24 to W.B., and the KL2 MeRIT award to O.C.A. from the Harvard Clinical and Translational Science Center (8KL2TR000168-05) and 1K22CA178269-01 from NIH, National Cancer Institute.

Resources provided to Martinos Center by the Center for Functional Neuroimaging Technologies, P41EB015896, a P41 Regional Resource supported by the National Institute of Biomedical Imaging and Bioengineering (NIBIB), National Institutes of Health. This work also involved the use of instrumentation supported by the NIH Shared Instrumentation Grant Program and/or High-End Instrumentation Grant Program; specifically, grant S10RR021110. MM acknowledges the support from Biotechnology Research Center (BTRC) grant P41 RR008079 and P41 EB015894, and NCC P30 NS076408.

References

Adalsteinsson E, Irarrazabal P, Topp S, Meyer C, Macovski A, Spielman DM. Volumetric spectroscopic imaging with spiral-based k-space trajectories. Magn Reson Med. 1998; 39:889–898. [PubMed: 9621912]

Agarwal N, Renshaw PF. Proton MR spectroscopy-detectable major neurotransmitters of the brain: biology and possible clinical applications. AJNR Am J Neuroradiol. 2012; 33:595–602. [PubMed: 22207303]

Andronesi OC, Gagoski BA, Adalsteinsson E, Sorensen AG. Correlation chemical shift imaging with low-power adiabatic pulses and constant-density spiral trajectories. NMR Biomed. 2012a; 25:195–209. [PubMed: 21774010]

Andronesi OC, Gagoski BA, Sorensen AG. Neurologic 3D MR Spectroscopic Imaging with Low-Power Adiabatic Pulses and Fast Spiral Acquisition. Radiology. 2012b; 262:647–661. [PubMed: 22187628]

Andronesi OC, Kim GS, Gerstner E, Batchelor T, Tzika AA, Fantin VR, Vander Heiden MG, Sorensen AG. Detection of 2-hydroxyglutarate in IDH-mutated glioma patients by in vivo spectral-editing and 2D correlation magnetic resonance spectroscopy. Sci Transl Med. 2012c; 4:116ra114.

Andronesi OC, Ramadan S, Mountford CE, Sorensen AG. Low-power adiabatic sequences for in vivo localized two-dimensional chemical shift correlated MR spectroscopy. Magn Reson Med. 2010a; 64:1542–1556. [PubMed: 20890988]

Andronesi OC, Ramadan S, Ratai EM, Jennings D, Mountford CE, Sorensen AG. Spectroscopic imaging with improved gradient modulated constant adiabaticity pulses on high-field clinical scanners. J Magn Reson. 2010b; 203:283–293. [PubMed: 20163975]

Arteaga de Castro CS, Boer VO, Andreychenko A, Wijnen JP, van der Heide UA, Luijten PR, Klomp DW. Improved efficiency on editing MRS of lactate and gamma-aminobutyric acid by inclusion of frequency offset corrected inversion pulses at high fields. NMR Biomed. 2013; 26:1213–1219. [PubMed: 23508792]

Baslow MH, Guilfoyle DN. Using proton magnetic resonance imaging and spectroscopy to understand brain “activation”. Brain Lang. 2007; 102:153–164. [PubMed: 16935326]

NIH-PA Author Manuscript NIH-PA Author Manuscript NIH-PA Author Manuscript

Benner T, Wisco JJ, van der Kouwe AJ, Fischl B, Vangel MG, Hochberg FH, Sorensen AG. Comparison of manual and automatic section positioning of brain MR images. Radiology. 2006; 239:246–254. [PubMed: 16507753]

Bhattacharyya PK, Lowe MJ, Phillips MD. Spectral quality control in motion-corrupted single-voxel J-difference editing scans: an interleaved navigator approach. Magn Reson Med. 2007; 58:808–812. [PubMed: 17899594]

Bilgic B, Gagoski B, Kok T, Adalsteinsson E. Lipid suppression in CSI with spatial priors and highly undersampled peripheral k-space. Magn Reson Med. 2013; 69:1501–1511. [PubMed: 22807147]

Bogner W, Gruber S, Doelken M, Stadlbauer A, Ganslandt O, Boettcher U, Trattnig S, Doerfler A, Stefan H, Hammen T. In vivo quantification of intracerebral GABA by single-voxel (1)H-MRS-How reproducible are the results? Eur J Radiol. 2010; 73:526–531. [PubMed: 19201120]

Bogner W, Gruber S, Trattnig S, Chmelik M. High-resolution mapping of human brain metabolites by free induction decay (1)H MRSI at 7 T. NMR Biomed. 2012; 25:873–882. [PubMed: 22190245]

Bogner W, Hess AT, Gagoski B, Tisdall MD, van der Kouwe AJ, Trattnig S, Rosen B, Andronesi OC. Real-time motion- and B0-correction for LASER-localized spiral-accelerated 3D-MRSI of the brain at 3T. Neuroimage. 2013; 88C:22–31. [PubMed: 24201013]

Choi IY, Lee SP, Merkle H, Shen J. In vivo detection of gray and white matter differences in GABA concentration in the human brain. Neuroimage. 2006; 33:85–93. [PubMed: 16884929]

Choi IY, Lee SP, Shen J. Selective homonuclear Hartmann-Hahn transfer method for in vivo spectral editing in the human brain. Magn Reson Med. 2005; 53:503–510. [PubMed: 15723418]

Deelchand DK, Henry PG, Marjańska M. Effect of carr-purcell refocusing pulse trains on transverse relaxation times of metabolites in rat brain at 9.4 Tesla. Magn Reson Med. 2014 Epub ahead of print. 10.1002/mrm.25088

Edden RA, Barker PB. Spatial effects in the detection of gamma-aminobutyric acid: improved sensitivity at high fields using inner volume saturation. Magn Reson Med. 2007; 58:1276–1282. [PubMed: 17969062]

Evans CJ, Puts NA, Robson SE, Boy F, McGonigle DJ, Sumner P, Singh KD, Edden RA. Subtraction artifacts and frequency (mis-)alignment in J-difference GABA editing. J Magn Reson Imaging. 2013; 38:970–975. [PubMed: 23188759]

Gao F, Edden RA, Li M, Puts NA, Wang G, Liu C, Zhao B, Wang H, Bai X, Zhao C, Wang X, Barker PB. Edited magnetic resonance spectroscopy detects an age-related decline in brain GABA levels. Neuroimage. 2013; 78:75–82. [PubMed: 23587685]

Henry ME, Lauriat TL, Shanahan M, Renshaw PF, Jensen JE. Accuracy and stability of measuring GABA, glutamate, and glutamine by proton magnetic resonance spectroscopy: a phantom study at 4 Tesla. J Magn Reson. 2011; 208:210–218. [PubMed: 21130670]

Henry PG, Dautry C, Hantraye P, Bloch G. Brain GABA editing without macromolecule contamination. Magn Reson Med. 2001; 45:517–520. [PubMed: 11241712]

Hess AT, Andronesi OC, Tisdall MD, Sorensen AG, van der Kouwe AJW, Meintjes EM. Real-time motion and B-0 correction for localized adiabatic selective refocusing (LASER) MRSI using echo planar imaging volumetric navigators. NMR Biomed. 2012; 25:347–358. [PubMed: 21796711]

Hess AT, Tisdall MD, Andronesi OC, Meintjes EM, van der Kouwe AJW. Real-Time Motion and B-0 Corrected Single Voxel Spectroscopy Using Volumetric Navigators. Magn Reson Med. 2011; 66:314–323. [PubMed: 21381101]

Hetherington HP, Newcomer BR, Pan JW. Measurements of human cerebral GABA at 4.1 T using numerically optimized editing pulses. Magn Reson Med. 1998; 39:6–10. [PubMed: 9438430]

Jensen JE, de Frederick BB, Renshaw PF. Grey and white matter GABA level differences in the human brain using two-dimensional, J-resolved spectroscopic imaging. NMR Biomed. 2005; 18:570–576. [PubMed: 16273508]

Kaiser LG, Young K, Matson GB. Elimination of spatial interference in PRESS-localized editing spectroscopy. Magn Reson Med. 2007; 58:813–818. [PubMed: 17899586]

Kaiser LG, Young K, Meyerhoff DJ, Mueller SG, Matson GB. A detailed analysis of localized J-difference GABA editing: theoretical and experimental study at 4 T. NMR Biomed. 2008; 21:22–32. [PubMed: 17377933]

NIH-PA Author Manuscript NIH-PA Author Manuscript NIH-PA Author Manuscript

Keating B, Ernst T. Real-time dynamic frequency and shim correction for single-voxel magnetic resonance spectroscopy. Magn Reson Med. 2012; 68:1339–1345. [PubMed: 22851160]

Keltner JR, Wald LL, Christensen JD, Maas LC, Moore CM, Cohen BM, Renshaw PF. A technique for detecting GABA in the human brain with PRESS localization and optimized refocusing spectral editing radiofrequency pulses. Magn Reson Med. 1996; 36:458–461. [PubMed: 8875418]

Keltner JR, Wald LL, Frederick BD, Renshaw PF. In vivo detection of GABA in human brain using a localized double-quantum filter technique. Magn Reson Med. 1997; 37:366–371. [PubMed: 9055226]

Kreis R. Issues of spectral quality in clinical H-1-magnetic resonance spectroscopy and a gallery of artifacts. NMR Biomed. 2004; 17:361–381. [PubMed: 15468083]

Lange T, Maclaren J, Buechert M, Zaitsev M. Spectroscopic imaging with prospective motion correction and retrospective phase correction. Magn Reson Med. 2012; 67:1506–1514. [PubMed: 22135041]

Mao J, Mareci TH, Andrew ER. Experimental study of optimal selective 180° radiofrequency pulses. J Magn Reson. 1988; 79:1–10.

Marjanska M, Lehericy S, Valabregue R, Popa T, Worbe Y, Russo M, Auerbach EJ, Grabli D, Bonnet C, Gallea C, Coudert M, Yahia-Cherif L, Vidailhet M, Meunier S. Brain dynamic neurochemical changes in dystonic patients: a magnetic resonance spectroscopy study. Mov Disord. 2013; 28:201–209. [PubMed: 23239076]

Maudsley AA, Domenig C, Govind V, Darkazanli A, Studholme C, Arheart K, Bloomer C. Mapping of brain metabolite distributions by volumetric proton MR spectroscopic imaging (MRSI). Magn Reson Med. 2009; 61:548–559. [PubMed: 19111009]

Mescher M, Merkle H, Kirsch J, Garwood M, Gruetter R. Simultaneous in vivo spectral editing and water suppression. NMR Biomed. 1998; 11:266–272. [PubMed: 9802468]

Michaeli S, Garwood M, Zhu XH, DelaBarre L, Andersen P, Adriany G, Merkle H, Ugurbil K, Chen W. Proton T2 relaxation study of water, N-acetylaspartate, and creatine in human brain using Hahn and Carr-Purcell spin echoes at 4T and 7T. Magn Reson Med. 2002; 47:629–633. [PubMed: 11948722]

Mullins PG, McGonigle DJ, O'Gorman RL, Puts NA, Vidyasagar R, Evans CJ, Edden RA. Current practice in the use of MEGA-PRESS spectroscopy for the detection of GABA. Neuroimage. 2014; 1:43–52. [PubMed: 23246994]

Muthukumaraswamy SD, Edden RA, Jones DK, Swettenham JB, Singh KD. Resting GABA concentration predicts peak gamma frequency and fMRI amplitude in response to visual stimulation in humans. Proc Natl Acad Sci U S A. 2009; 106:8356–8361. [PubMed: 19416820]

Near J, Evans CJ, Puts NA, Barker PB, Edden RA. J-difference editing of gamma-aminobutyric acid (GABA): simulated and experimental multiplet patterns. Magn Reson Med. 2013; 70:1183–1191. [PubMed: 23213033]

Northoff G, Walter M, Schulte RF, Beck J, Dydak U, Henning A, Boeker H, Grimm S, Boesiger P. GABA concentrations in the human anterior cingulate cortex predict negative BOLD responses in fMRI. Nat Neurosci. 2007; 10:1515–1517. [PubMed: 17982452]

Novotny EJ Jr, Fulbright RK, Pearl PL, Gibson KM, Rothman DL. Magnetic resonance spectroscopy of neurotransmitters in human brain. Ann Neurol. 2003; 54(Suppl 6):S25–31. [PubMed: 12891651]

Pan JW, Duckrow RB, Spencer DD, Avdievich NI, Hetherington HP. Selective homonuclear polarization transfer for spectroscopic imaging of GABA at 7T. Magn Reson Med. 2013; 69:310–316. [PubMed: 22505305]

Petroff OA. GABA and glutamate in the human brain. Neuroscientist. 2002; 8:562–573. [PubMed: 12467378]

Petroff OA, Hyder F, Collins T, Mattson RH, Rothman DL. Acute effects of vigabatrin on brain GABA and homocarnosine in patients with complex partial seizures. Epilepsia. 1999; 40:958–964. [PubMed: 10403220]

Posse S, Tedeschi G, Risinger R, Ogg R, Le Bihan D. High speed 1H spectroscopic imaging in human brain by echo planar spatial-spectral encoding. Magn Reson Med. 1995; 33:34–40. [PubMed: 7891533]

NIH-PA Author Manuscript

NIH-PA Author Manuscript

NIH-PA Author Manuscript

Pouwels PJ, Brockmann K, Kruse B, Wilken B, Wick M, Hanefeld F, Frahm J. Regional age dependence of human brain metabolites from infancy to adulthood as detected by quantitative localized proton MRS. Pediatr Res. 1999; 46:474–485. [PubMed: 10509371]

Provencher SW. Automatic quantitation of localized in vivo 1H spectra with LCModel. NMR Biomed. 2001; 14:260–264. [PubMed: 11410943]

Puts NA, Edden RA. In vivo magnetic resonance spectroscopy of GABA: a methodological review. Prog Nucl Magn Reson Spectrosc. 2012; 60:29–41. [PubMed: 22293397]

Roemer PB, Edelstein WA, Hayes CE, Souza SP, Mueller OM. The NMR phased array. Magn Reson Med. 1990; 16:192–225. [PubMed: 2266841]

Rothman DL, Petroff OA, Behar KL, Mattson RH. Localized 1H NMR measurements of gamma-aminobutyric acid in human brain in vivo. Proc Natl Acad Sci U S A. 1993; 90:5662–5666. [PubMed: 8516315]

Smith SA, Levante TO, Meier BH, Ernst RR. Computer Simulations in Magnetic Resonance. An Object-Oriented Programming Approach. J Magn Reson A. 1994; 106:75–105.

Terpstra M, Henry PG, Gruetter R. Measurement of reduced glutathione (GSH) in human brain using LCModel analysis of difference-edited spectra. Magn Reson Med. 2003; 50:19–23. [PubMed: 12815674]

Terpstra M, Ugurbil K, Gruetter R. Direct in vivo measurement of human cerebral GABA concentration using MEGA-editing at 7 Tesla. Magn Reson Med. 2002; 47:1009–1012. [PubMed: 11979581]

Thomas MA, Hattori N, Umeda M, Sawada T, Naruse S. Evaluation of two-dimensional L-COSY and JPRESS using a 3 T MRI scanner: from phantoms to human brain in vivo. NMR Biomed. 2003; 16:245–251. [PubMed: 14648883]

Thomas MA, Yue K, Binesh N, Davanzo P, Kumar A, Siegel B, Frye M, Curran J, Lufkin R, Martin P, Guze B. Localized two-dimensional shift correlated MR spectroscopy of human brain. Magn Reson Med. 2001; 46:58–67. [PubMed: 11443711]

Tisdall MD, Hess AT, Reuter M, Meintjes EM, Fischl B, van der Kouwe AJW. Volumetric navigators for prospective motion correction and selective reacquisition in neuroanatomical MRI. Magn Reson Med. 2012; 68:389–399. [PubMed: 22213578]

van der Kouwe AJ, Benner T, Salat DH, Fischl B. Brain morphometry with multiecho MPRAGE. Neuroimage. 2008; 40:559–569. [PubMed: 18242102]

van der Kouwe AJW, Benner T, Fischl B, Schmitt F, Salat DH, Harder M, Sorensen AG, Dale A. On-line automatic slice positioning for brain MR imaging. Neuroimage. 2005; 27:222–230. [PubMed: 15886023]

Waddell KW, Avison MJ, Joers JM, Gore JC. A practical guide to robust detection of GABA in human brain by J-difference spectroscopy at 3 T using a standard volume coil. Magn Reson Imaging. 2007; 25:1032–1038. [PubMed: 17707165]

Xin L, Gambarota G, Mlynarik V, Gruetter R. Proton T2 relaxation time of J-coupled cerebral metabolites in rat brain at 9.4 T. NMR Biomed. 2008; 21:396–401. [PubMed: 17907262]

Zaitsev M, Speck O, Hennig J, Buchert M. Single-voxel MRS with prospective motion correction and retrospective frequency correction. NMR Biomed. 2010; 23:325–332. [PubMed: 20101605]

Zhu H, Edden RA, Ouwerkerk R, Barker PB. High resolution spectroscopic imaging of GABA at 3 Tesla. Magn Reson Med. 2011; 65:603–609. [PubMed: 21337399]

NIH-PA Author Manuscript

NIH-PA Author Manuscript

NIH-PA Author Manuscript

Highlights

- MEGA-LASER provided >1.66 times larger GABA signal integral than MEGA-PRESS
- MEGA-LASER was insensitive to B_1+ and chemical shift related artifacts
- Real-time position and B0 updates with selective reacquisition reduced subtraction artifacts in MEGA-editing
- Spiral encoding allowed 3D mapping of GABA+ in the same time as normally required for single-voxel MRS

NIH-PA Author Manuscript

NIH-PA Author Manuscript

NIH-PA Author Manuscript

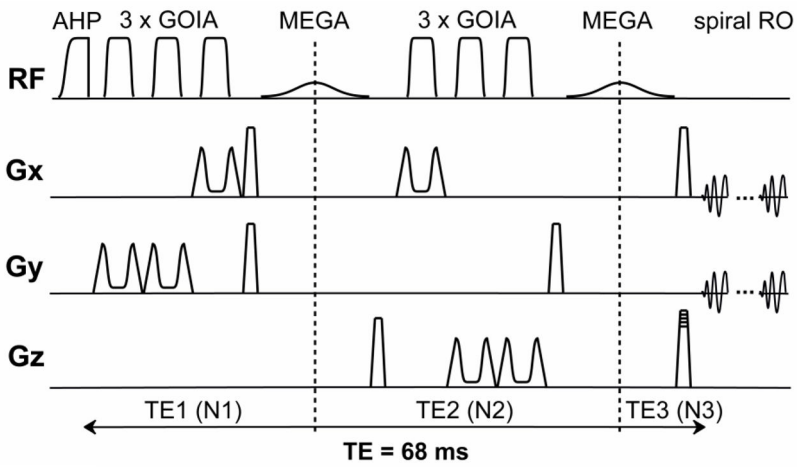

Fig. 1.

Sequence schema of the MEGA-LASER sequence with 3D acquisition weighted stack of spirals encoding. Full adiabatic selection is provided by an AHP excitation pulse and three pairs of spatially-selective GOIA-W(16,4) refocusing pulses. Two frequency-selective Gauss refocusing pulses and adjacent spoiler gradients are used for MEGA editing. Phase encoding gradients in the z-direction are superimposed on top of the last MEGA spoiler. Constant-density spiral readout encode the x,y-plane. Preceding water suppression and volumetric navigator modules are not shown.

NIH-PA Author Manuscript
NIH-PA Author Manuscript
NIH-PA Author Manuscript

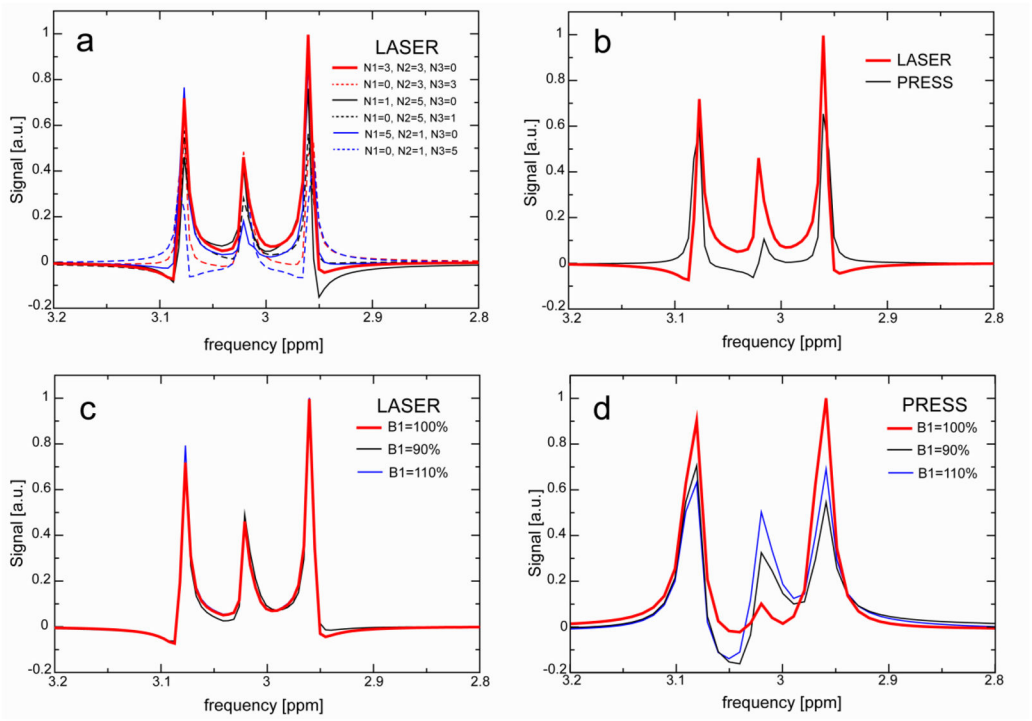

Fig. 2.

Simulations for the GABA triplet at 3.01 ppm as observed in the subtraction spectra of the MEGA-LASER and MEGA-PRESS sequences. (a) Comparison of the effects of different positions and time intervals of the MEGA pulses in the MEGA-LASER sequence on the spectral appearance of the edited 3ppm GABA triplet. The MEGA pulses divide the total TE in three intervals (i.e., TE1/TE2/TE3 which include N1/N2/N3 GOIA pulses). The highest edited signal was obtained when the MEGA pulses were separated by half of the echo time (TE2=34 ms) in the second part of the echo (i.e., N1=3; N2=3; N3=0). (b) MEGA-LASER achieves ~2 times higher integrated GABA signal amplitude than MEGA-PRESS. The change in the GABA triplet pattern due to ±10% change in B1+ field was significantly smaller for (c) MEGA-LASER (3–7%) than for (d) MEGA-PRESS (12–28%). Slice profiles for PRESS and LASER pulses are shown in Supplementary Fig. 1.

NIH-PA Author Manuscript

NIH-PA Author Manuscript

NIH-PA Author Manuscript

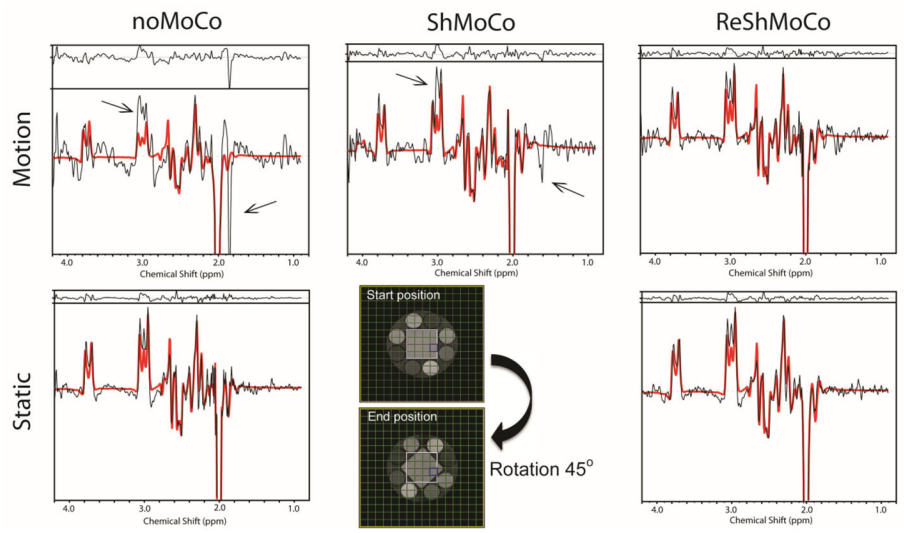

Fig. 3.

A cylindrical multi-compartment localization phantom (rotated by 45° around its axis) was used to illustrate the performance of the motion correction methods implemented in the MEGA-LASER sequence. The center of the sphere contains a rectangular compartment of 5×5×5 cm^3 containing brain metabolites at close to physiological concentrations. The central compartment was surrounded by eight Falcon tubes filled with 10% ethanol or water mixed with Gd-DTPA to have enough image contrast to be traceable during motion.

LCModel fits of five sample MEGA-edited spectra are displayed for the same voxel positioned inside the multi-compartment localization phantom (indicated by blue square). The top row (“motion”) shows LCmodel fits of spectra for data that were acquired during phantom movement. The bottom row (“static”) shows spectra obtained without phantom movement. The left column shows results without any correction (“noMoCo”), the center an example for using only B_0 shim and motion correction (“ShMoCo”), and the right column shows results, when selective reacquisition is used in addition to B_0 shim and motion correction (“ReShMoCo”).

Spectra obtained during static condition without correction and with ReShMoCo correction were comparable. Spectra obtained during motion were significantly corrupted, if no correction was performed, and significantly improved when using ShMoCo. Further improvement in spectral quality was observed when using ReShMoCo.

Substantial subtraction artifacts and contamination from signal outside the VOI are indicated by arrows. Plots of motion tracking are shown in Supplementary Fig. 2.

NIH-PA Author Manuscript

NIH-PA Author Manuscript

NIH-PA Author Manuscript

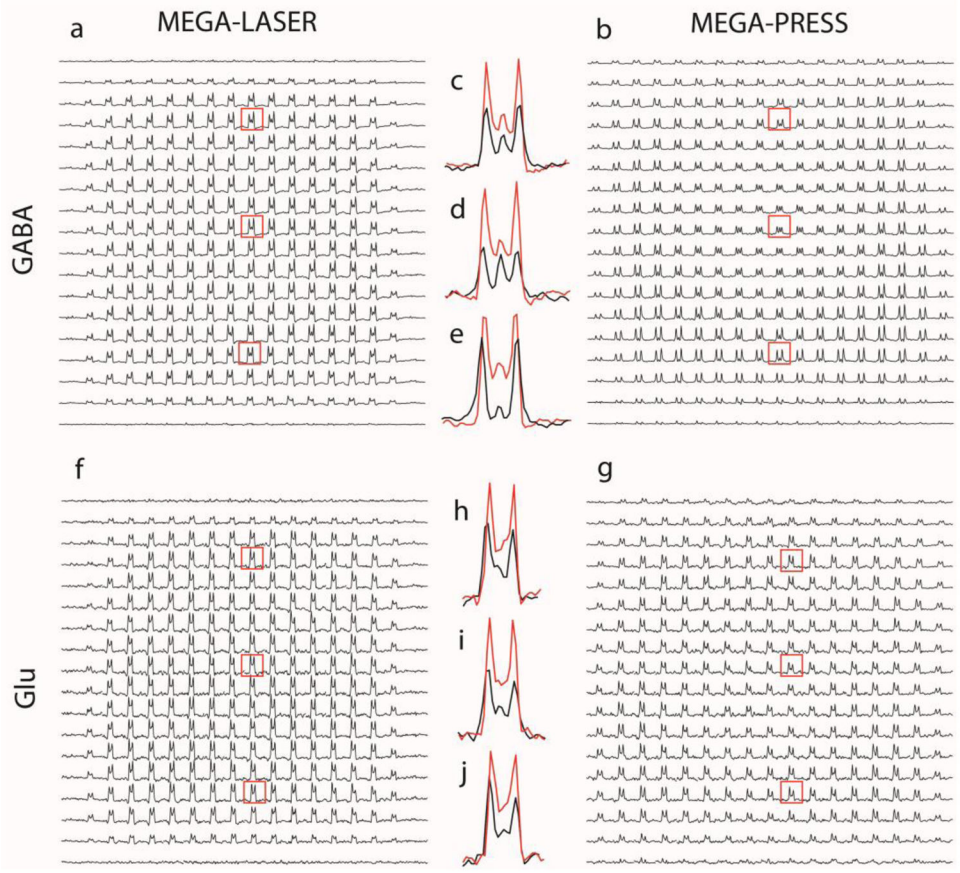

Fig. 4.

Spectral grids illustrating the spatial heterogeneity of the subtracted GABA triplet (a–e) and Glu doublet (f–j) pattern that is observable in the central transversal slice obtained from a homogeneous spherical phantom (diameter 16 cm; 20 mM GABA and 20mM Glu solution). The B_1^+ inhomogeneity was similar to conditions found *in vivo* (85±9° inside VOI). MEGA-editing via (a,f) LASER was compared to (b,g) PRESS using 3D-MRSI (FOV 20×20×16 cm^3; VOI 10×10×6 cm^3; matrix 20×20×16 interpolated to 32×32×16). The grid clearly shows improved spatial VOI selection for (a,f) MEGA-LASER compared to (b,g) MEGA-PRESS. Three representative spectra were selected from each grid (red rectangular boxes; c,h-top; d,i-center; e,j-bottom) for a direct comparison between MEGA-LASER (red lines) and MEGA-PRESS (black lines). In particular, they illustrate: (c) reduced GABA/Glu signal amplitude in PRESS due to the 4-compartment effect in the anterior direction; (d) altered signal intensity ratio between inner-to-outer GABA resonance lines due to too high B_1^+ in the center of the phantom; and (e) lower GABA/Glu signal integral for MEGA-PRESS compared to MEGA-LASER even under ideal conditions. The overall GABA signal integral within the VOI (excluding border voxels) was 1.66 times larger for MEGA-LASER (in a.u. 43±5) than for MEGA-PRESS (26±5). For certain voxels the changes in the subtracted GABA integral were even larger (~2). Similar behavior can be observed for Glu. Note: Identical scaling was used for MEGA-LASER and MEGA-PRESS, but different scaling between GABA and Glu. A 6 Hz exponential filter was applied for display purposes.

NIH-PA Author Manuscript

NIH-PA Author Manuscript

NIH-PA Author Manuscript

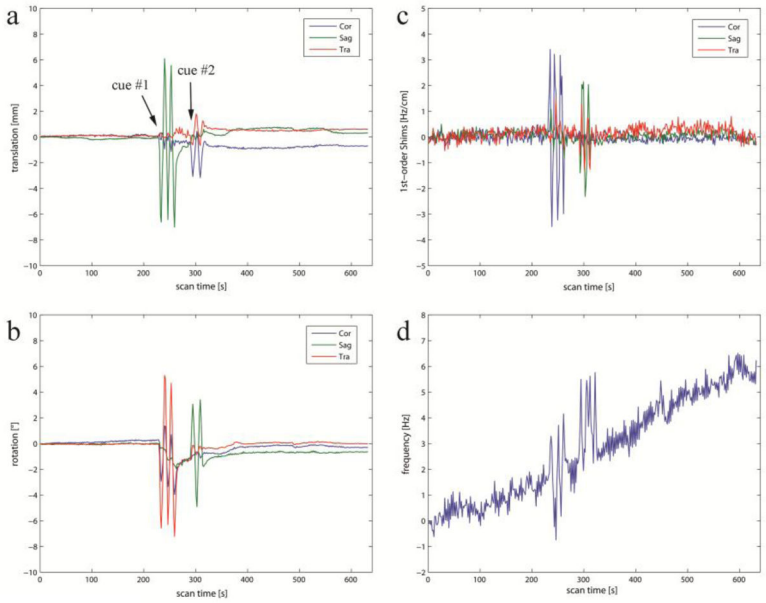

Fig. 5.

(a) Translation, (b) rotation, (c) first-order shim terms, and (d) frequency changes, as determined by the vNav and corrected during the 3D-MRSI scan (10×10×10 matrix) are plotted as a function of measurement time in the scanner coordinate system. The scan time of ~8 min was prolonged by ~2 min due to necessary reacquisition of corrupted data. During the scan, two different motion tasks were performed by the volunteer: (1) repeated head rotation in the transversal plane (right-left); and (2) repeated head rotation in the sagittal plane (up-down). Frequency changes shown in (d) illustrate the combined effect of head motion and scanner instability-related frequency drift.

NIH-PA Author Manuscript
NIH-PA Author Manuscript
NIH-PA Author Manuscript

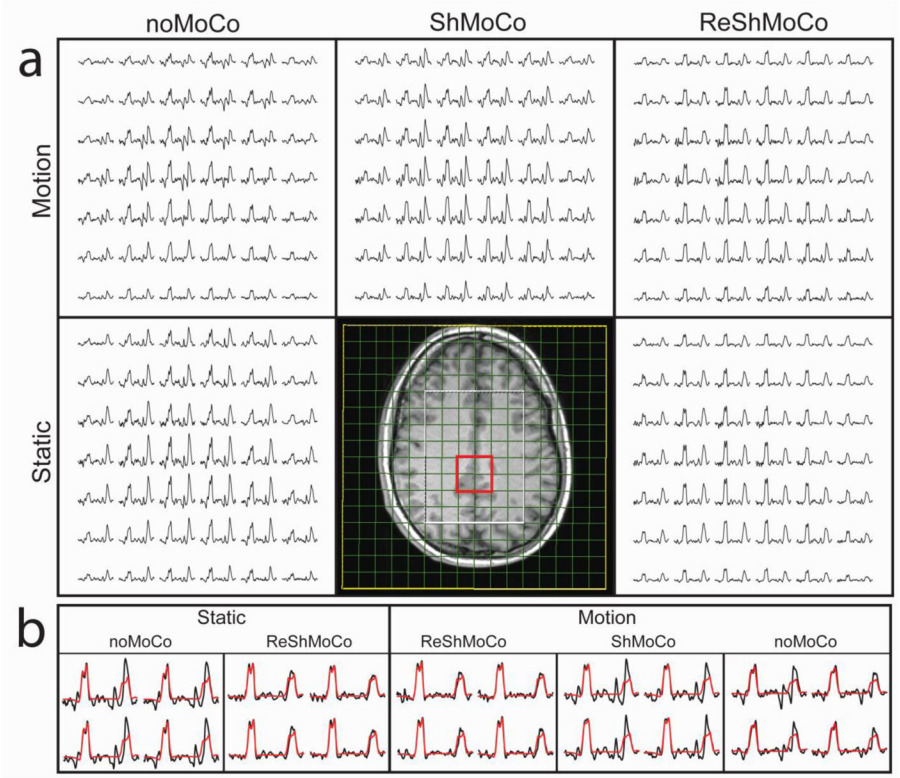

Fig. 6.

Five stacks of subtraction spectra of volunteer number 5 showing the frequency range from 2.8–4.2 ppm containing Glx (left signal at ~3.8ppm) and GABA+ (right signal at ~3ppm) for the VOI (see white rectangular box inside the brain) of a central transversal slice obtained via a 3D-MEGA-LASER acquisition with an 8 cm^3 isotropic resolution in a healthy volunteer. In (a), the top row ("motion") shows stacks of spectra for data that were acquired, while the subject was performing a head motion task. The bottom row ("static") shows stacks of spectra obtained, while the subject was instructed not to move. The left column shows results without any correction ("noMoCo"), the center an example for using only B_0 shim and motion correction ("ShMoCo"), and the right column shows results, when selective reacquisition is used in addition to B_0 shim and motion correction ("ReShMoCo"). Without correction both static and motion scans were affected by subtraction artifacts. There was a lot of scanner instability causing subtraction artifacts even in the static uncorrected case. ShMoCo alone did not fully eliminate subtraction artifacts. In comparison, ReShMoCo significantly increased spectral quality for the static and even more in the motion case. (b) Sample LCModel fitting for spectra from the posterior cingulate (position indicated by red square) for all five different motion and correction methods. Note – the same scaling was used for all spectra and 3 Hz exponential filtering was applied to reduce noise level only for visualization purpose.

NIH-PA Author Manuscript

NIH-PA Author Manuscript

NIH-PA Author Manuscript

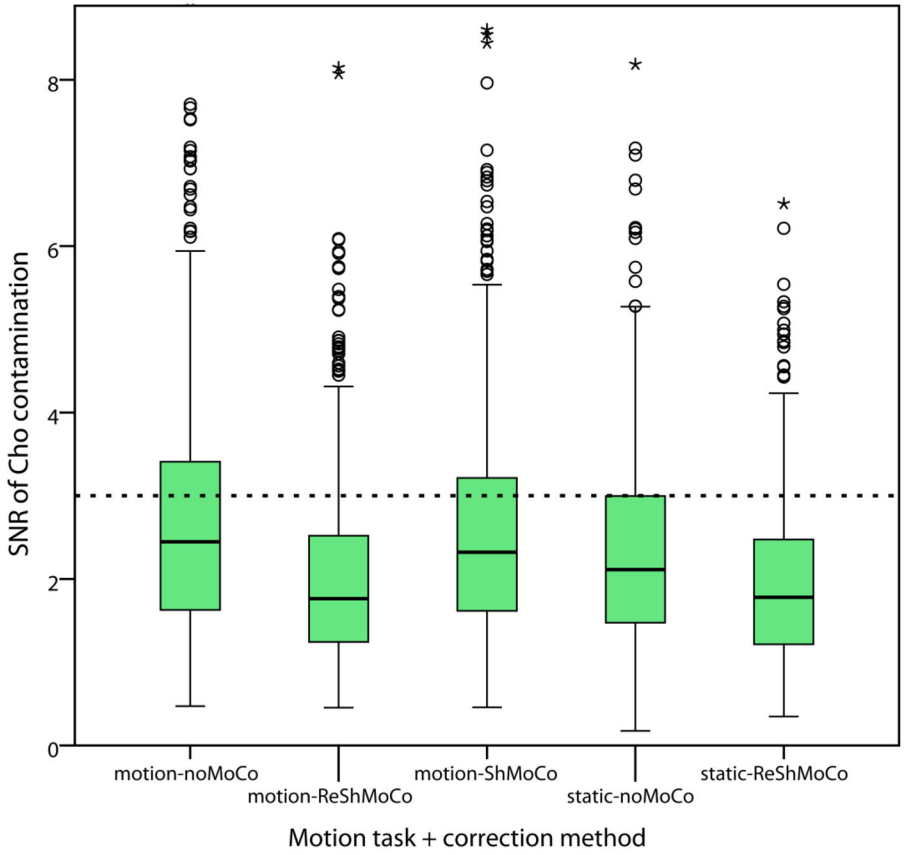

Fig. 7.

Box plot illustrating the SNR of subtraction artifacts at ~3.2 ppm (Cho) of all spectra inside the VOI mask as a measure of contamination for different combinations of motion tasks and correction methods (i.e., motion task with no motion correction; motion task with shim- and motion correction; motion task with reacquisition, shim- and motion correction; static head position with no motion correction; and static head position with reacquisition, shim- and motion correction). An SNR threshold of SNR=3 was defined to filter contamination that can be considered noise. Only contamination with SNR > 3 was considered substantial and further processed.

NIH-PA Author Manuscript
NIH-PA Author Manuscript
NIH-PA Author Manuscript

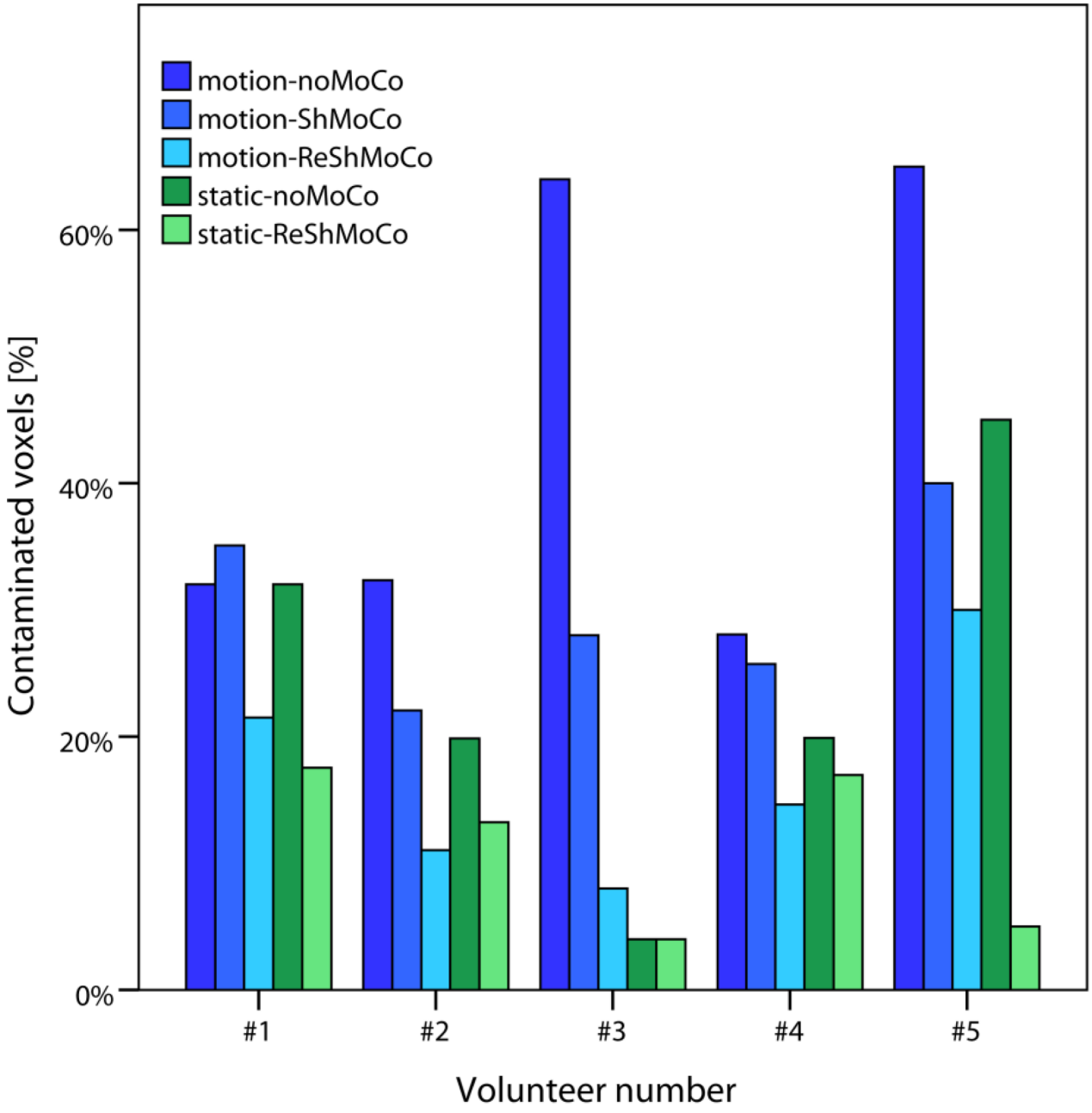

Fig. 8.

Percentage of contaminated voxels (i.e., defined as SNR of Cho subtraction artifact > 3) within the investigated mask displayed for all five volunteers (Vol#1–5) and for different combinations of motion tasks and correction methods (i.e., motion task with no motion correction; motion task with shim- and motion correction; motion task with reacquisition, shim- and motion correction; static head position with no motion correction; and static head position with reacquisition, shim- and motion correction). Scans with ReShMoCo had significantly lower percentage of contaminated voxels than ShMoCo or no correction.

NIH-PA Author Manuscript

NIH-PA Author Manuscript

NIH-PA Author Manuscript

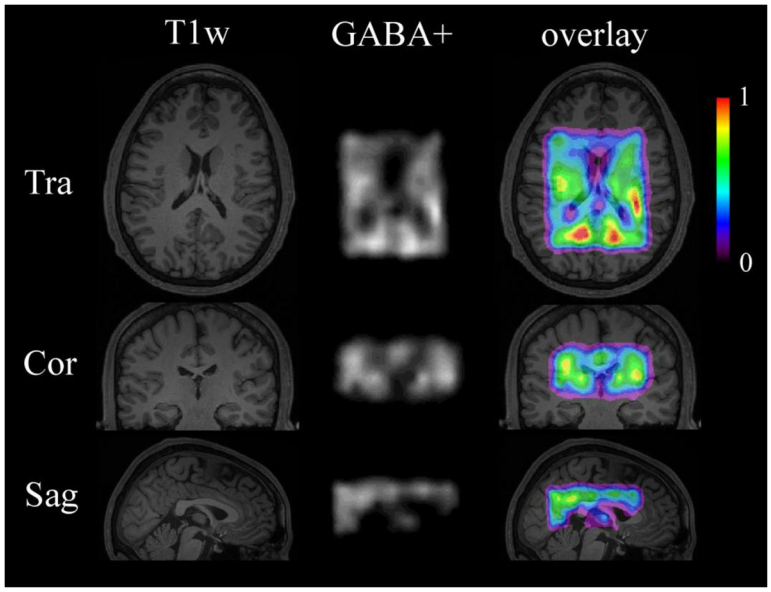

Fig. 9.

Morphological T1-weighted reference images (left), 3D GABA+ maps obtained by MEGA-LASER and ReShMoCo in a healthy volunteer with 1 cm^3 isotropic resolutions in ~24 min (center), and color-coded overlay (right) displayed in transversal, sagittal, and coronal plane. For display purposes GABA+ maps were interpolated to the T_1-weighted MRI. The contours of the ventricles, as well as increased GABA+ levels in regions that predominantly contain grey matter are well visible on the 3D GABA+ maps as visible from direct comparison with morphological reference images. Detailed imaging parameters are listed in table 1.

NIH-PA Author Manuscript

NIH-PA Author Manuscript

NIH-PA Author Manuscript

Table 1

Sample 3D MEGA-LASER MRSI protocols ranging from short standard (low) resolution mapping of GABA+ and Glx (protocol I) over moderate resolution (protocol II) to longer high-resolution mapping (protocol III).

Protocol #	**I**	**II**	**III**
TR (ms)	1600	1600	1600
TE (ms)	68	68	68
nominal resolution (cm^3)	8	3	1
matrix	10×10×10	14×14×14	20×20×20
interpolated matrix	16×16×16	16×16×16	32×32×32
FOV (mm^3)	200×200×200	200×200×200	200×200×200
VOI (mm^3)	110×90×50	110×90×50	110×90×50
bandwidth (kHz)	1.1	1.25	1.25
temp. interleaves	2	2	2
angular interleaves	1	2	4
phase cycle	2-step	2-step	2-step
editing pulse	Gauss - 60 Hz	Gauss - 60 Hz	Gauss - 60 Hz
averages	16	10	4
scan time (min)	8:13	15:54	24

NIH-PA Author Manuscript NIH-PA Author Manuscript NIH-PA Author Manuscript

Table 2

Comparison of spectral quality parameters inside the VOI (i.e., SNR, CRLB, GABA+/Glx signal intensity ratio, contamination) for difference spectra of *in vivo* scans in five healthy volunteers. All volunteers were instructed to either stay still (static) or perform a predefined movement of their head (motion). In total, five scans were performed in each subject: (a) a static scan without any correction (noMoCo); (b) a static scan with reacquisition, shim-, and motion correction (ReShMoCo); (c) a motion-affected scan with noMoCo; (d) a motion-affected scan with only shim-, and motion correction (ShMoCo); and (e) a motion-affected scan with full ReShMoCo. ReShMoCo substantially improved the quality of subtraction spectra. The estimates for the static and motion ReShMoCo scans are the closest (bolded).

	Static		**Motion**		
	noMoCo	**ReShMoCo**	**noMoCo**	**ShMoCo**	**ReShMoCo**
GABA+ SNR	12.6±5.0	**11.9±5.3**	13.3±5.9	12.7±5.6	**11.2±4.8**
GABA+ CRLB [%]	11.6±3.3	**9.9±3.1**	12.4±3.6	11.5±3.38	**10.2±3.0**
GABA+/Glx	0.86±0.09	**0.82±0.06**	0.87±0.08	0.84±0.08	**0.81±0.08**
Cont. SNR	2.4±1.2	**2.0±1.0**	2.8±1.6	2.6±1.5	**2.0±1.2**